EFFECT OF MAGNETITE AND CHITOSAN-MAGNETITE ADDITION ON BACTERIAL LEVELS AND NH_3-N (FREE-LIVING N_2-FIXING BACTERIA CULTURE)

Ali Umar[1], Deden Saprudin[1*], Fahrizal Hazra[2]
[1]Department of Chemistry, Faculty of Mathematics and Natural Sciences, IPB University, Jl. Tanjung Kampus IPB Dramaga, Bogor 16680, West Java, Indonesia
[2]Department of Soil Science and Land Resource, Faculty of Agriculture, IPB University, Jl. Meranti Kampus IPB Dramaga, Bogor 16680, West Java, Indonesia
[*]Email: dsp@apps.ipb.ac.id

Received 16 July 2023
Accepted 24 October 2023

Abstract

Free-living N_2-fixing bacteria are essential in the soil because they provide a source of nitrogen in the form of ammonium needed by plants to be used in building protein blocks. The fixation of free N_2 needs to be increased by adding nanomaterials such as magnetite (Fe_3O_4), which has an active group and can be a source of nitrogenase enzyme cofactor. In this study, increased N_2 fixation used N_2-fixing bacteria in Burks medium. This increase was determined by measuring NH_3 levels using the Phenate method formed after Burks medium was treated with Fe_3O_4 and chitosan-magnetite (CS-Fe_3O_4). The study found that the number of bacteria can be well decreased. This research showed that using Fe_3O_4 and CS-Fe_3O_4 increased NH_3-N levels in cultures of free-living nitrogen-fixing bacteria by 15.40% and 75.54%. For future development, it can be in the form of optimization, the effect of adding the same material to plant secondary metabolites, and the mechanism of bacteria in using the material.

Keywords*: bacteria, chitosan, composite, Fe_3O_4, NH_3-N*

Introduction

Nanotechnology has a wide range of applications in agriculture. Some nanoparticles boost crop yield by improving germination, photosynthetic activity, and metabolites such as proteins and nitrogen-containing compounds (Feng *et al.*, 2022; Huang *et al.*, 2015). According to Kacprzak et al., (2022) Bacterial activity is critical to both terrestrial and oceanic ecosystems. Bacteria decompose dead organisms in order to release nutrients back into the environment. The number of bacteria in the environment must be controlled to prevent biological pollution. Bacterial activity plays a vital role in the ecosystem. Nitrogenase enzymes in free-living N_2-fixing bacteria catalyze the conversion of atmospheric N_2 gas to ammonia (Aasfar *et al.*, 2021; Smercina *et al.*, 2019). *Rhizobium* will fix N_2 from the atmosphere by invading plant roots through fine roots (Shimkets, 2015). Bacteria without a symbiotic relationship with plants (free-living bacteria) are commonly used in organic fertilizers (Jacoby *et al.*, 2017).

Rivani *et al.*, (2019) define magnetite (Fe_3O_4) as a magnetic iron oxide with a cubic inverse spinel structure and oxygen. Chitosan coats Fe_3O_4 by forming contacts between functional groups on the surface (CS-Fe_3O_4) (Htwe *et al.*, 2022). The addition of Fe_3O_4 to bacteria is intended as a source of cofactors to increase ammonia production. Regulations for the number of bacteria in organic fertilizers have been established. The number of viable microbes is 1×10^5 CFU ml^{-1}

(Mentan RI, 2019). Biotechnology employs molybdenum, vanadium, cobalt, and iron to aid N_2-fixing bacteria.

The carboxyl and amino groups in peptidoglycan on the bacterial wall are abundant. At neutral pH, this results in a negative and positive charge. The negative charge can form bonds with magnetite. As a result, bacteria can bind to Fe_3O_4 and reduce the bacterial population. The fixation of free nitrogen from the air causes the NH_3 fixation process to run because of an enzyme nitrogenase. This enzyme is a protein that contains vitamins and minerals. The nitrogenase enzyme is sensitive to oxygen. The nitrogen fixation process will be hampered if the media contains too much nitrogen. The use of magnetite will stimulate the production of NH_3. According to relevant studies, the hydrothermal approach produces Fe_3O_4, easily soluble in water. As a result, Fe_3O_4 can be employed as an enzyme cofactor as a source of Fe (in the form of ions) (Majeed *et al.*, 2013). Although this study did not use Fe_3O_4, which is easily soluble in water, and with the knowledge base from previous studies examining the effect of adding Fe_3O_4 on Nitrogen content in N_2-fixing bacteria bound to root nodules, this is the first step to study the effect of adding Fe_3O_4 and its composite form to NH_3-N in free-living nitrogen-fixing bacteria, which is novel. The benefit of this research is determining the level of bacteria and application to produce NH_3-N from free-living N2-fixing in liquid samples after applying Fe_3O_4 and CS-Fe_3O_4.

Research Methods

Materials

The materials used in this study were distilled water (dH_2O), double-distilled water (ddH_2O), $FeCl_3.6H_2O$ (EMSURE® Merck, Germany), $FeSO_4.7H_2O$ (Merck, Germany), NaOH (EMSURE® Merck, Germany), ethanol (EMSURE® Merck, Germany), commercial chitosan, CH_3CO_2H, KBr, K_2HPO_4 (Cica, Kanto, Japan), KH_2PO_4, $MgSO_4.7H_2O$ (Merck, Germany), $CaCl_2.2H_2O$ (Wako, Japan), $NaMoO_4.2H_2O$ (Merck, Germany), D-(-)Mannitol, technical agar, sucrose (Merck, Germany), pure isolate of N_2-fixing bacteria (Agensia Hayati), NaCl 0.85%, NH_4Cl, liquified phenol, $Na_2[Fe(CN)_5NO].2H_2O$ (Merck, Germany), trisodium citrate, NaOCl, purple crystal (HiMedia), iodine-gram (HiMedia), and safranin (HiMedia).

Instrumentation

The equipment used in this study were a measuring flask, beaker, Erlenmeyer, test tube, vial, funnel, Petri dish, magnetic stirrer-heater, external magnet, oven, micropipette (and tip), ose needle, autoclave, laminar flow cabinet, fume hood, microscope, FTIR (PerkinElmer Spectrum One), XRD (Rigaku Minifex), SEM-EDX (Thermoscientific: Quanta 650 SEM), and UV-Vis Instrument (Genesys 10S).

Procedure

1) Fe_3O_4 and CS-Fe_3O_4 synthesis (Hariani *et al.*, 2013; Pham *et al.*, 2016)
   13.1718 g $FeCl_3.6H_2O$ and 7.4277 g $FeSO_4.7H_2O$ were dissolved in 50 ml of dH_2O each. Then, the solution was mixed and stirred for 60 minutes at 30 °C. A total of 1 M NaOH 250 ml was added to the mixture (drop by drop) at 70 °C for 5 hours. The formed particles (black Fe_3O_4) were then separated using an external magnet and washed using dH_2O and ethanol to be dried in an oven at 60–70 °C. To synthesize CS-Fe_3O_4, 0.5033 g of chitosan was dissolved in 100 ml of 2% CH_3CO_2H. Then, the 1.3346 g Fe_3O_4 (phase water) was added to chitosan solution drop by drop while stirred at high speed. CS-Fe_3O_4 was then separated using an external magnet and washed using deionized water. The particles were dried in an oven at 60 °C.

2) Fe_3O_4 and CS-Fe_3O_4 characterizations and data processing
   a. Fourier Transform Infrared (FTIR)
      A dry KBr was prepared and inserted with a small sample into a press to make a KBr plate. The formed plate was inserted into the FTIR machine and applied at wavenumbers 4000 cm^{-1} to 450 cm^{-1}. The data obtained were plotted on OriginLab software.
   b. X-Ray Diffraction (XRD)
      The sample was X-Ray diffraction at a wavelength of 1.541874 Å with 2θ 3–90°.
   c. Scanning Electron Microscopy-Energy Dispersive X-Ray (SEM-EDX)
      Sample surface images were taken using an SEM device with magnification up to 20,000×, and dispersive energy was measured and plotted in OriginLab software.
3) Nitrogen-free media (NFM) and Burks media preparation
   The medium was prepared by adding ingredients to dH_2O following the composition in Table 1. The media was sterilized using an autoclave at a pressure of 0.1 MPa for 20 minutes.

Table 1. Addition of materials to create media

Materials	Addition (g)
NFM Media (400 ml dH_2O)	
K_2HPO_4	0.3593
KH_2PO_4	0.0425
$MgSO_4.7H_2O$	0.0438
$CaCl_2.2H2O$	0.0404
$NaMoO_4.2H_2O$	0.0035
$FeSO_4.7H_2O$	0.0050
D-(-)Mannitol	2.0119
Agar	10.4201
Burks Media (250 ml dH_2O)	
K_2HPO_4	0.0524
KH_2PO_4	0.1996
$MgSO_4.7H_2O$	0.0505
$CaCl_2.2H_2O$	0.0328
$NaMoO_4.2H_2O$	0.0039
$FeCl_3.6H_2O$	0.0055
Sucrose	5.0008

4) Preparation of cultivation of bacteria, bacteria-Fe_3O_4, and bacteria-CS-Fe_3O_4
   The pure isolate of N_2-fixing bacteria (purchased through e-commerce) was rejuvenated on Burks media for 72 hours. A total of 25 g isolates each on Burks media were added separately; no treatment (0), 0.25 g Fe3O4 (A), and 0.25 g CS-Fe3O4 (B) were added. The sample was then centrifuged for 10 minutes hours at 3000 rpm.
5) Bacterial enumeration with Total Plate Count-Pour Plate method
   0, A, and B samples were diluted serially. Aseptically, each sample was pipetted of 0.1 ml and put into 9.9 ml of physiological salt NaCl 0.85%/diluent blank ($1:10^2$). The sample was then shaken using a vortex, taking as much as 0.1 ml, and inserted into a 9.9 ml diluent blank ($1:10^4$). At the stage of dilution 10^4 times, as much as 1 ml of sample was taken and put into 9 ml of diluent blanks to obtain a dilution of $1:10^5$ (C), and as much as 0.1 ml then put into 9.9 ml of diluent blanks to get a dilution of $1:10^6$ (D).

Sample C was taken as much as 1 ml, 2× (1:50000), and 0.1 ml ($1:10^6$). Each was inserted into a Petri dish that contained the medium. D samples were taken as much as 1 ml, 2× (1:500000), and 0.1 ml ($1:10^7$). The inoculum was poured sterilely on Petri dishes that contained the medium. After the medium became solid, the Petri dish was placed upside down to incubate at 30 °C for 72 hours. The colonies formed were then counted (the calculable colonies are 25–250 CFU). Colonies were calculated at observance of serial dilution.

6) NH_3-N determination on bacteria culture

25 g of Burks media each were added separately; no treatment (0*), 0.25 g Fe3O4 (Y), and 0.25 g CS-Fe3O4 (Z) were added. The bacteria were grown aseptically on the medium and incubated for 48 hours. The culture grown on the medium was centrifuged at 3000 rpm for 10 minutes. A total of 11.1 ml of phenol (> 89%) was mixed with 95% ethanol to a volume of 100 ml. Then $Na_2[Fe(CN)_5NO].2H_2O$ solution was prepared by adding 0.5 g of $Na_2[Fe(CN)_5NO].2H_2O$ to 100 ml of ddH_2O water. The oxidizing solution was prepared by dissolving 50 g of trisodium citrate and 2.5 g of NaOH in 250 ml of ddH_2O water. The 100 ml mixture was mixed with 25 ml of 12% NaOCl.

A 100 ppm NH_4Cl stock solution was prepared by weighing 0.3819 g (previously dried at 100 °C for 2 hours) and adding ddH_2O up to 1 L. 5 ml was taken and added to a 100 ml measuring flask using ddH_2O (5 ppm). From a stock of 5 ppm NH_4Cl, it was pipetted and added to a 50 ml measuring flask using ddH_2O to obtain 0 (absorbance correction), 0.001, 0.01, 0.1, 0.2, and 0.6 ppm as the final concentration. A total of 0.2 ml of the formed supernatant was mixed with 1 ml of phenol solution, 1 ml of $Na_2[Fe(CN)_5NO].2H_2O$ solution, and 2.5 ml of oxidizing agent solution, then added ddH_2O water up to 50 ml. The apparent color change was determined using spectrophotometry at a wavelength of 640 nm using a standard curve of 0.001–0.6 ppm ammonium chloride.

7) Gram Staining

The culture tube was shaken until the suspension was evenly distributed. Aseptically the bacterial suspension was applied to the center of the top surface of the glass object using an inoculated loupe wire. Then, spread evenly over the area provided. The smear was allowed to air dry, and heat fixation was carried out.

The glass of the object was flooded by the primary dye, purple crystals, for 1 minute, and the remaining substance was rinsed with water from an aqueous bottle. Then, smear the bacteria flooded with iodine grams for 2 minutes. The spread was washed using 96% ethanol as a bleach for 30 seconds. After draining, the smear was flooded with a counter-dye, safranin, for 30 seconds. The remaining dye was rinsed using water. Glass objects were observed using a microscope at 400× and 1000× magnifications.

Results and Discussion

Results of synthesis and characterization of Fe_3O_4 and CS-Fe_3O_4

Nanoscience, according to Mulvaney (2015), is the manipulation of particles and atomic structures to create materials with nanoscale properties. Fe_3O_4 can be used as a separation technology, protein immobilization, catalysis, and environmental science. It can be synthesized using various methods (Liu *et al.*, 2020). Fe_3O_4 is synthesized using the coprecipitation method in an alkaline environment. The reaction involves the addition of ferrous and ferric ions to a base of NaOH. Fe_3O_4 is formed by reacting Fe^{2+} and Fe^{3+} ions (Jannah and

Onggo, 2019). In its clumps, Fe_3O_4 can form chemical bonds with organic or inorganic molecules. The negative partial charge at -OH will bind to the positive partial charge of chitosan. Chitosans are added to the aqueous phase of Fe_3O_4 to coat it (Shaumbwa *et al.*, 2021).

The FTIR spectra of synthetic Fe_3O_4 and CS-Fe_3O_4, as well as the commercial chitosan, are shown in Figure 1. The properties of Fe_3O_4 are investigated through the FTIR spectrum, which reveals that the absorption bands at 1624 and 3433 cm^{-1} as -OH on the surface of Fe_3O_4 and at 575 cm^{-1} as Fe-O (Li *et al.*, 2015; Zhang *et al.*, 2013). FTIR analysis of CS-Fe_3O_4 reveals 3457 cm^{-1} as -NH_2 and -OH, 1634 cm^{-1} -C=O, 1422 cm^{-1} -CH_2, 1047 cm^{-1} -C-O-C, and 564 cm^{-1} Fe-O. The peak of Fe-O shifts towards a smaller wavenumber, indicating Fe_3O_4 is coated with chitosan. (Ates *et al.*, 2018). In commercial chitosan, the absorption bands of 3423 cm^{-1} are -NH_2 and -OH, 2928 cm^{-1} -CH, 1637 cm^{-1} -C=O, 1417 cm^{-1} -CH_2, and 1022 cm^{-1} -C-O-C.

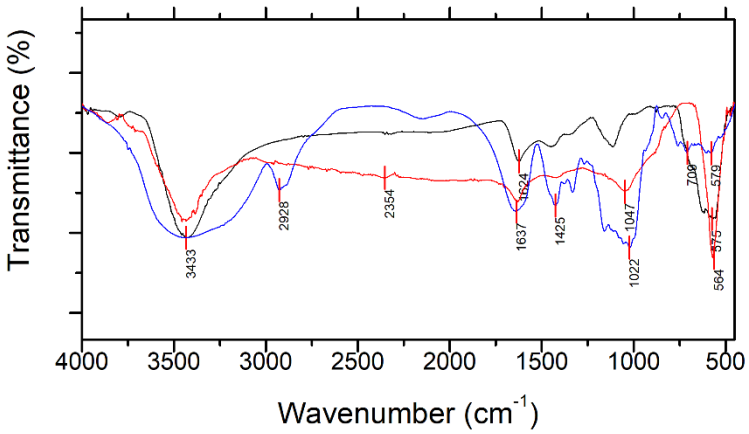

Figure 1. FTIR spectra of synthesized Fe_3O_4 (black), CS-Fe_3O_4 (red), and CS (blue)

XRD was used to examine the crystal structures of synthetic Fe_3O_4 and CS-Fe_3O_4. Figure 2 shows the diffractogram. The diffraction peaks at 220, 311, 400, 422, and 440 are characteristic of Fe_3O_4. This peak is compared to ICSD database no. 53412 and reveals that particles form close to the tops of existing databases. Differences in peaks on the CS-Fe_3O_4 diffractogram indicate differences in the crystal composition and structure.

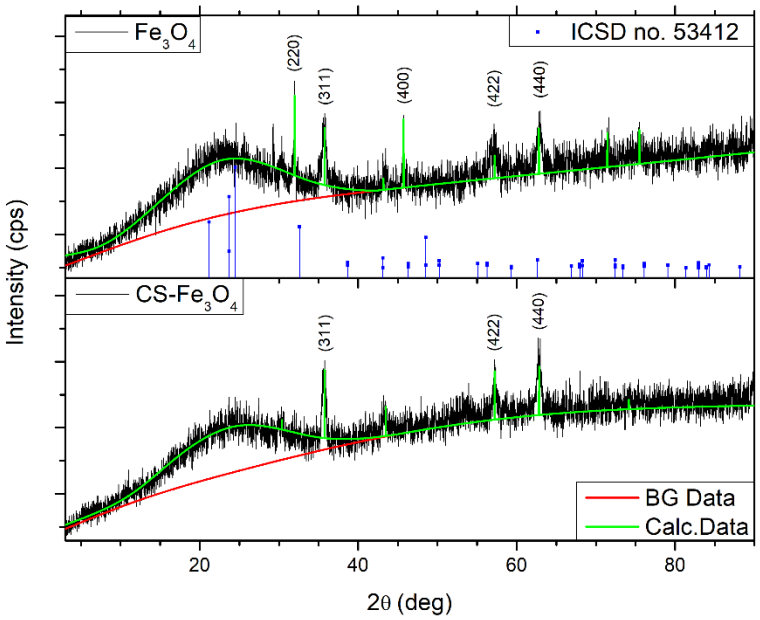

Figure 2. Diffractogram on synthesized Fe_3O_4 and CS-Fe_3O_4 versus Fe_3O_4 card (ICSD number 53412)

The synthesized Fe_3O_4 and CS-Fe_3O_4 morphology was examined using SEM at a magnification of 5000× (Figure 3). Particles of CS-Fe_3O_4 appear more degraded or distributed in SEM pictures than Fe_3O_4. SEM pictures from the literature are used as a reference and compared (Figure 4). After chitosan administration, the surface of Fe_3O_4 particles changed completely, indicating morphological differences between Fe_3O_4 and CS-Fe_3O_4.

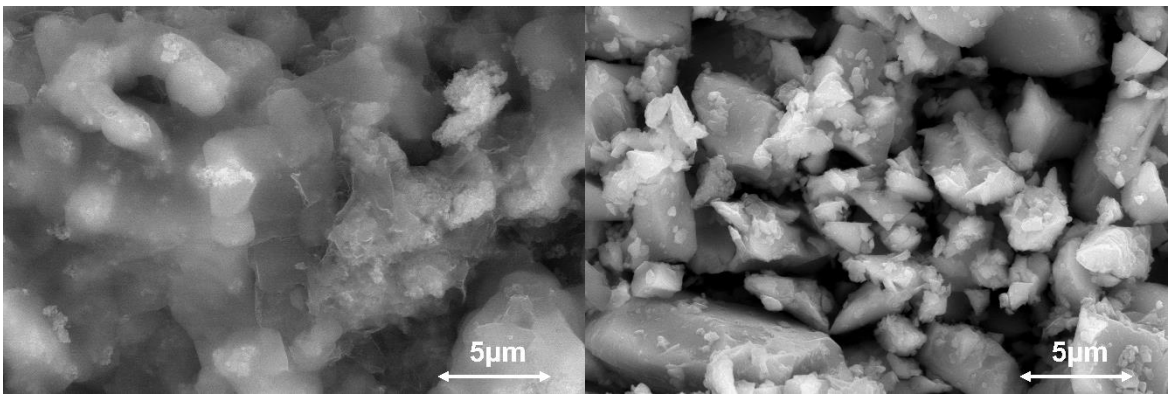

Figure 3. SEM images of synthesized Fe_3O_4 (left) and CS-Fe_3O_4 (right)

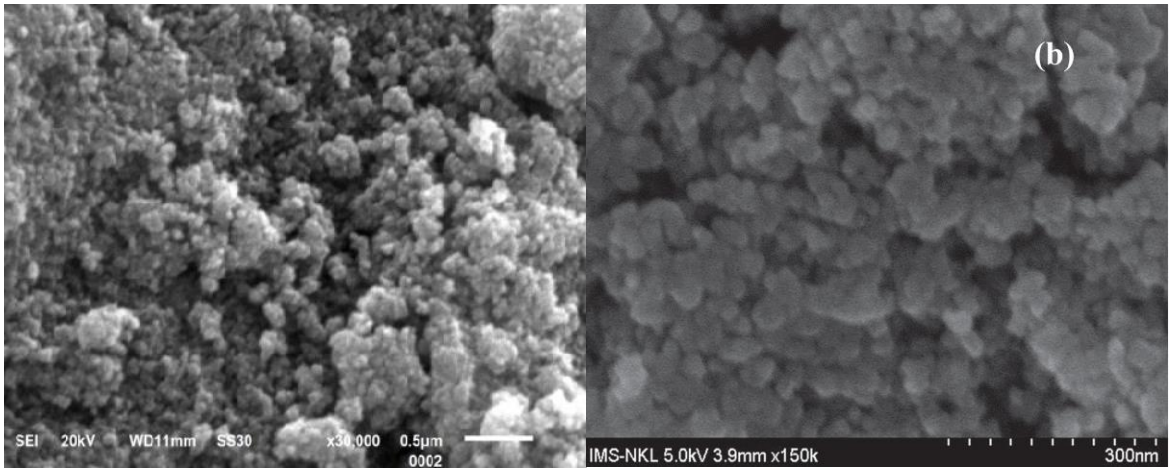

Figure 4. Fe_3O_4 (left) and CS-Fe_3O_4 (right) SEM image literature (Hariani *et al.*, 2013; Pham *et al.*, 2016)

The EDX spectra (Figure 5) show strong peaks in Fe and O. The Fe_3O_4 components formed have a 70.2% Fe and a 26.8% O composition. Al impurities account for up to 0.6%. In the composition of CS-Fe_3O_4, the components formed are 64.4% Fe, 24.6% O, 8.4% C, 1.5% N, and 0.9% Al, according to the findings (Ates *et al.*, 2018). The peak of Al is visible because Al is carried away when weighing $FeCl_3$, which is corrosive to aluminum plates. The peak C source in the EDX Fe_3O_4 spectra can be attributed to material contact with the carbon source during preparation and analysis. However, the background of SEM-EDX is higher than TEM-EDX's, allowing the C peak to be observed at more than 2%. The SATW window on EDX contains a transmission profile with a significant absorption edge immediately above but very close to the X-ray energy C (to detect Be), resulting in a peak at the energy point C. Unlike the TEM-EDX, the specimen material lacks a C peak because distinctive X-rays dominate the spectra.

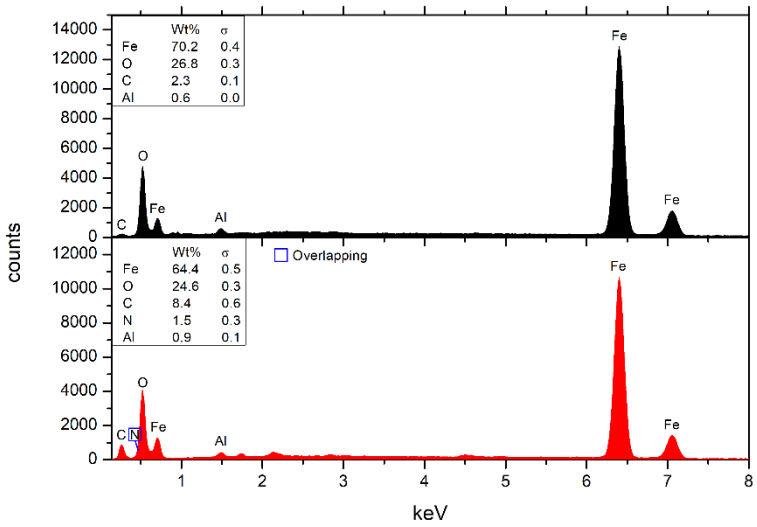

Figure 5. EDX spectra of synthesized Fe_3O_4 (black) and CS-Fe_3O_4 (red)

Bacterial growth using Total Plate Count and Gram Staining

Free-living N_2-fixing bacteria can grow in substrates high in carbohydrates but lacking nitrogen. Burks media is used to rejuvenate pure isolates. Other bacteria cannot bind to N_2, preventing them from growing on the substrates. Bacteria are treated with Fe_3O_4 to grow on Burks and NFM media. Bacterial immobilization is the physical confinement/absorption of microbial cells into a specific region of space, Fe_3O_4, to inhibit bacterial cell movement. This confinement process is caused by the clumping of fluid phase solutes (bacteria) on the surface of Fe_3O_4. The microbial cell can be physically confined through cohesive forces (Martins *et al.*, 2013; Kharissova *et al.*, 2014).

Colonies formed in samples of 0* with no treatment were in the calculation range of 25 to 250 colonies. Table 2 shows the colonies that formed. The number of colonies that can be counted is between 25 and 250. Number of colonies formed in samples A and B was below statistical confidence. The number of bacteria in each sample was calculated using general calculations. Sample 0 indicates an average number of bacteria was 3.2×10^6 ml^{-1}, while samples A and B show an estimate of bacteria of less than 1.25×10^6 ml^{-1}. This shows a decrease in the number of bacteria when given Fe_3O_4 (A) and CS-Fe_3O_4 (B) versus no treatment (0). Although the values are less than the LoQ, the data shows that colonies formed are greater than LoD, implying that sample treatment with CS-Fe_3O_4 results in a lower colony value. This suggests that treatment with CS-Fe_3O_4 results in a lower colony value. Reliability (ISO 14661-2) was acceptable for all dilution factors in 0, A, and B plate count samples.

Table 2. Colonies formed on nitrogen-free media

Dilution factor	Sample code					
	0		A		B	
	Colonies formed (CFU)					
	Repetition					
	1	2	1	2	1	2
1:50000	64	60	14	7[a]	3[a]	8[a]
1:500000	10[a]	12[a]	5[a]	2[a]	3[a]	2[a]
10^{-6}	8[a]	6[a]	1[a]	2[a]	1[a]	1[a]
10^{-7}	3[a]	2[a]	0[a]	0[a]	0[a]	0[a]
N	3.2×10^6		$< 1.25 \times 10^{6*}$		$< 1.25 \times 10^{6*}$	

[a]Do not have a statistically significant number of colonies

*Estimated plate count

Figure 6 depicts the morphology of bacteria under a microscope after gram staining. Gram staining reveals the color of violet crystals attached to the bacterial wall, indicating gram-positive bacteria. Bacteria are rod-shaped, and some form chains (filaments) when they assemble.

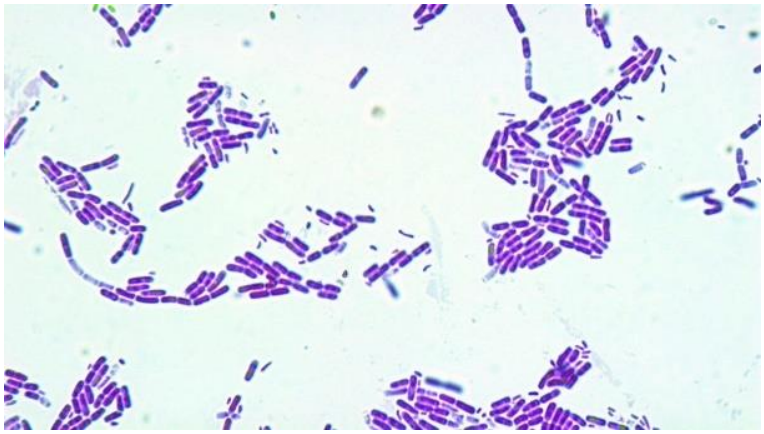

Figure 6. Colonies formed under a microscope after gram staining

Determination of NH_3-N

According to Jiménez-Vicente *et al.*, (2018) and Tanabe and Nishibayashi, (2019), when Mo is scarce, N_2 fixation will take on genetically distinct forms. The V-nitrogen fixation and alternative nitrogen fixation (Anf) systems replace Mo with Fe. The alternative enzymes are made up of two separable protein components. Bacteria that fix N_2 using nitrogenase enzymes via Mo. The phenate test is used to determine the NH_3-N content in samples using the Bethelot reaction (Li *et al.*, 2020). There are several techniques for determining the concentration of NH_3-N in a sample. The phenate tests are used to test for the presence of the element in the sample.

As transient species, phenol and chloroamine create radical pairs. The phenate's negative charge on oxygen stabilizes cation species and forms the structure of benzoquinone. In the last stage, phenate has a single electron transfer pathway to synthesize blue indophenol. In this experiment, sodium nitroprusside was utilized as a catalyst. The absorbance of the sample was compared to the standard absorbance to determine the NH_3-N content. The NH_3-N concentration range of the standard curve used in the experiment is 0 (as a blank), 0.001, 0.01, 0.1, 0.2, and 0.6 ppm, with linear equation $y = 1.33583x + 0.01484$ and linearity $R^2 = 0.96419$.

A total of 0.2 ml of samples were collected to be determined using the phenate method, the absorbance was measured, and the concentration value was determined using the provided equation. The concentration list is then calculated, taking into account the dilution factor. The average concentration of NH_3-N in sample 0* was 0.08917 ± 0.09040 ppm with an accuracy of 89.45%, in sample Y 0.10290 ± 0.01146 ppm with an accuracy of 88.87%, and in sample Z 0.15653 ± 0.01143 ppm with an accuracy of 92.70% (Table 3).

Table 3. NH3-N concentration in the sample

Sample	Repetition	NH_3-N (ppm) in 0.2 ml sample (x)	Absorbance	NH_3-N (ppm) in 1 ml sample
0*	1	0.01958	0.041	0.09790
	2	0.01584	0.036	0.07920
	3	0.01808	0.039	0.09040
		$\bar{x}$		0.08917
		σ		0.00941
		Accuracy		89.45%
Y	1	0.02108	0.043	0.10540
	2	0.01808	0.039	0.09040
	3	0.02258	0.045	0.11290
		$\bar{x}$		0.10290
		σ		0.01146
		Accuracy		88.87%
Z	1	0.03380	0.060	0.16900
	2	0.02931	0.054	0.14655
	3	0.03081	0.056	0.15405
		$\bar{x}$		0.15653
		σ		0.01143
		Accuracy		92.70%

Changes in concentration from samples that were not given and given treatment were visualized using an average plot with standard error as an error. There is an increase in concentration formed after treatment (Figure 7). When the sample was given Fe_3O_4, the rise in NH_3-N was 15.40% compared to the control (no treatment); when the sample was given CS-Fe_3O_4, the increase was 75.54% compared to the control. When given CS-Fe_3O_4, the growth was 52.19% more than when given Fe_3O_4.

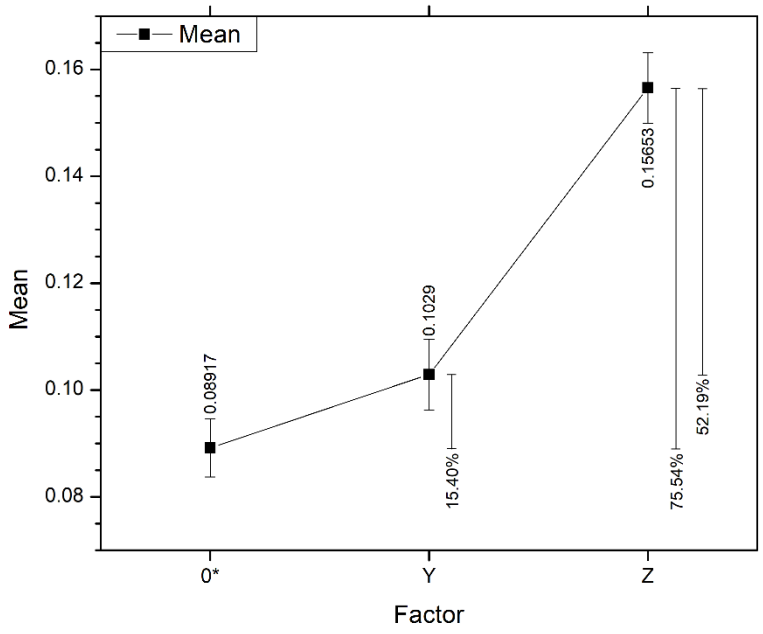

Figure 7. Means plot (SE as error) the concentration of NH_3-N

The One Way ANOVA test and Tukey test were performed to see significant differences between treatments. Pairs of samples are performed by the Tukey test. The null hypothesis is means that all levels are equal, and the alternative hypothesis is means that one or more levels are different. The value of Prob > F at a confidence level of 0.05 is < 0.05 (≈ 0.006), indicating the rejection of the null hypothesis and drawing the conclusion that several levels have significant mean differences.

Table 3. Colonies formed on nitrogen-free media

Descriptive statistics				
Sample	**Sample Size**	**Mean**	**Standard Deviation**	**SE of Mean**
0*	3	0.08917	0.00941	0.00543
Y	3	0.10290	0.01146	0.00661
Z	3	0.15653	0.01143	0.00660

One Way ANOVA					
Sample	**DF**	**Sum of Squares**	**Mean Square**	**F Value**	**Prob > F**
Model	2	0.00760	0.00380	32.5452	6.012×10^{-4}
Error	6	7.0088×10^{-4}	1.1681×10^{-4}		
Total	8	0.00830			

Pairs of samples are performed by the Tukey test. The sig value of 1 indicates a significant difference in the means at level 0.05, and 0 indicates that the mean has no significant difference at level 0.05. The Tukey test concludes that at 0.05, the mean significant difference occurred in samples Z 0* (given CS-Fe_3O_4 and not given) and Z Y (given CS-Fe_3O_4 and Fe_3O_4).

Table 4. Colonies formed on nitrogen-free media

Tukey test								
Sample pair	**MeanDiff**	**SEM**	**q Value**	**Prob**	**Alpha**	**Sig**	**LCL**	**UCL**
Y 0*	0.0137	0.0088	2.2009	0.3328	0.05	0	-0.0133	0.0408
Z 0*	0.0674	0.0088	10.7959	6.4×10^{-4}	0.05	1	0.0403	0.0944
Z Y	0.0536	0.0088	8.5951	0.0022	0.05	1	0.0266	0.0807

Rhizobium symbiotic performance in conventional peanut plants is consistent with previous research (De Souza-Torres *et al.*, 2021). The finding investigated Rhizobium symbiotic performance in conventional peanut plants (increased enzyme activity by 51.2–90.7%) (Table 5). The study found a significant difference at level 0.05 in CS-Fe_3O_4 and Fe_3O_4 activity levels.

Table 5. Effects of Fe3O4 use on nitrogenase activity and leghaemoglobin content in Rhizobium inoculation (De Souza-Torres *et al.*, 2021)

Parameter	Nitrogenase activity (µmol C_2H_4 h^{-1} $plant^{-1}$)	Leghaemoglobin content (mg g^{-1} FW nodules)	%increase
Fe_3O_4	6.5 ± 0.07	3.04 ± 0.05	51.2%
Rhizobium inoculation	6.8 ± 0.04	3.01 ± 0.01	58.1%
Fe_3O_4 + *Rhizobum* inoculation	8.2 ± 0.05	3.8 ± 0.08	90.7%
Control	4.3 ± 0.03	2.1 ± 0.04	

Rui et al., (2016) investigated the potential of iron oxide as an iron fertilizer in *Arachis hypogaea* plants in a related study. These iron oxide particles stimulate plant development by modulating phytohormone levels and antioxidant enzyme activity. According to the same source, iron oxide is absorbed into soil sand to improve the availability of Fe to plants.

Conclusions

From this study, the authors can conclude that using Fe_3O_4 and CS-Fe_3O_4 in pure isolates of N_2-fixing bacteria decreases the number of bacteria that can grow and increase the levels of synthesized NH_3-N. Some things need further research, such as an increase in NH_3-N formed in specific bacteria and the mechanism of bacteria using Fe_3O_4 and CS-Fe_3O_4 as a source of cofactors in nitrogenase enzymes. The follow-up action in connection with this study is that plant metabolites are formed when given fertilizer containing N_2-fixing bacteria that have modified conditions in Fe_3O_4 and CS-Fe_3O_4. Furthermore, a study on the optimal settings of numerous factors is required to provide good NH_3 levels for plants.

Acknowledgment

The authors would like to thank the Department of Chemistry and the Department of Soil Science and Land Resources IPB University, who helped in this experiment.

Conflicts of Interest

The authors report no conflicts of interest relevant to this article.

Authors Contributions

Ali Umar provided research funding, conducted experiments, processed data, and wrote scripts. This research was supervised by Deden Saprudin and Fahrizal Hazra.

References

Aasfar, A., Bargaz, A., Yaakoubi, K., Hilali, A., Bennis, I., Zeroual, Y. and Meftah Kadmiri, I., 2021. Nitrogen Fixing *Azotobacter* Species as Potential Soil Biological Enhancers for Crop Nutrition and Yield Stability. *Frontiers in Microbiology*, 12.

Ates, B., Ulu, A., Köytepe, S., Ali Noma, S.A., Kolat, V.S. and Izgi, T., 2018. Magnetic-propelled Fe_3O_4 –chitosan carriers enhance l-asparaginase catalytic activity: a promising strategy for enzyme immobilization. *RSC Advances*, 8(63), pp.36063–36075.

Feng, Y., Kreslavski, V.D., Shmarev, A.N., Ivanov, A.A., Zharmukhamedov, S.K., Kosobryukhov, A., Yu, M., Allakhverdiev, S.I. and Shabala, S., 2022. Effects of Iron Oxide Nanoparticles (Fe_3O_4) on Growth, Photosynthesis, Antioxidant Activity and Distribution of Mineral Elements in Wheat (Triticum aestivum) Plants. *Plants*, 11(14), p.1894.

Hariani, P.L., Faizal, M., Ridwan, R., Marsi, M. and Setiabudidaya, D., 2013. Synthesis and Properties of Fe_3O_4 Nanoparticles by Co-precipitation Method to Removal Procion Dye. *International Journal of Environmental Science and Development*, 4(3), pp.336–340.

Htwe, A.T., Maung, M.T.M. and Naing, Z., 2022. Synthesis of chitosan-coated magnetite nanoparticles using co-precipitation method for copper(II) ions removal in aqueous solution. *World Journal of Engineering*, 19(5), pp.726–734.

Huang, S., Wang, L., Liu, L., Hou, Y. and Li, L., 2015. Nanotechnology in agriculture, livestock, and aquaculture in China. A review. *Agronomy for Sustainable Development*, 35(2), pp.369–400.

Indonesia, M.P.R., 2019. Persyaratan Teknis Minimal Pupuk Organik, Pupuk Hayati, dan Pembenah Tanah.

Jacoby, R., Peukert, M., Succurro, A., Koprivova, A. and Kopriva, S., 2017. The Role of Soil Microorganisms in Plant Mineral Nutrition—Current Knowledge and Future Directions. *Frontiers in Plant Science*, 8, p.1617.

Jannah, N.R. and Onggo, D., 2019. Synthesis of Fe_3O_4 nanoparticles for colour removal of printing ink solution. *Journal of Physics: Conference Series*, 1245(1), p.12040.

Jiménez-Vicente, E., Martin Del Campo, J.S., Yang, Z.-Y., Cash, V.L., Dean, D.R. and Seefeldt, L.C., 2018. Chapter Nine - Application of affinity purification methods for analysis of the nitrogenase system from *Azotobacter vinelandii*. In: Armstrong, F., (ed.) *Methods in Enzymology*. Enzymes of Energy Technology. Academic Press, pp. 231–255.

Kacprzak, M., Malińska, K., Grosser, A., Sobik-Szołtysek, J., Wystalska, K., Dróżdż, D., Jasińska, A. and Meers, E., 2022. Cycles of carbon, nitrogen and phosphorus in poultry manure management technologies – environmental aspects. *Critical Reviews in Environmental Science and Technology*, 0(0), pp.1–25.

Kharissova, O. V, Dias, H.V.R. and Kharisov, B.I., 2014. Magnetic adsorbents based on micro- and nano-structured materials. *RSC Advances*, 5(9), pp.6695–6719.

Li, D., Xu, X., Li, Z., Wang, T. and Wang, C., 2020. Detection methods of ammonia nitrogen in water: A review. *TrAC Trends in Analytical Chemistry*, 127, p.115890.

Li, S., Zhang, T., Tang, R., Qiu, H., Wang, C. and Zhou, Z., 2015. Solvothermal synthesis and characterization of monodisperse superparamagnetic iron oxide nanoparticles. *Journal of Magnetism and Magnetic Materials*, 379, pp.226–231.

Liu, S., Yu, B., Wang, S., Shen, Y. and Cong, H., 2020. Preparation, surface functionalization and application of Fe_3O_4 magnetic nanoparticles. *Advances in Colloid and Interface Science*, 281, p.102165.

Majeed, M.I., Lu, Q., Yan, W., Li, Z., Hussain, I., Tahir, M.N., Tremel, W. and Tan, B., 2013. Highly water-soluble magnetic iron oxide (Fe_3O_4) nanoparticles for drug delivery: enhanced in vitro therapeutic efficacy of doxorubicin and MION conjugates. *Journal of Materials Chemistry B*, 1(22), p.2874.

Martins, S.C.S., Martins, C.M., Fiúza, L.M.C.G. and Santaella, S.T., 2013. Immobilization of microbial cells: A promising tool for treatment of toxic pollutants in industrial wastewater. *African Journal of Biotechnology*, 12(28).

Mulvaney, P., 2015. Nanoscience vs Nanotechnology—Defining the Field. *ACS Nano*, 9(3), pp.2215–2217.

Pham, X.N., Nguyen, T.P., Pham, T.N., Tran, T.T.N. and Tran, T.V.T., 2016.

Synthesis and characterization of chitosan-coated magnetite nanoparticles and their application in curcumin drug delivery. *Advances in Natural Sciences: Nanoscience and Nanotechnology*, 7(4), p.45010.

Rivani, D.A., Retnosari, I., Kusumandari and Saraswati, T.E., 2019. Influence of TiO_2 addition on the magnetic properties of carbon-based iron oxide nanocomposites synthesized using submerged arc-discharge. *IOP Conference Series: Materials Science and Engineering*, 509, p.012034.

Rui, M., Ma, C., Hao, Y., Guo, J., Rui, Y., Tang, X., Zhao, Q., Fan, X., Zhang, Z., Hou, T. and Zhu, S., 2016. Iron Oxide Nanoparticles as a Potential Iron Fertilizer for Peanut (*Arachis hypogaea*). *Frontiers in Plant Science*, 7.

Shaumbwa, V.R., Liu, D., Archer, B., Li, J. and Su, F., 2021. Preparation and application of magnetic chitosan in environmental remediation and other fields: A review. *Journal of Applied Polymer Science*, 138(42).

Shimkets, L.J., 2015. Development, Prokaryotic: Variety and Versatility☆. In: *Reference Module in Biomedical Sciences*. Elsevier.

Smercina, D.N., Evans, S.E., Friesen, M.L. and Tiemann, L.K., 2019. To Fix or Not To Fix: Controls on Free-Living Nitrogen Fixation in the Rhizosphere. *Applied and Environmental Microbiology*, 85(6).

De Souza-Torres, A., Govea-Alcaide, E., Gómez-Padilla, E., Masunaga, S.H., Effenberger, F.B., Rossi, L.M., López-Sánchez, R. and Jardim, R.F., 2021. Fe_3O_4 nanoparticles and Rhizobium inoculation enhance nodulation, nitrogen fixation and growth of common bean plants grown in soil. *Rhizosphere*, 17, p.100275.

Tanabe, Y. and Nishibayashi, Y., 2019. Recent advances in nitrogen fixation upon vanadium complexes. *Coordination Chemistry Reviews*, 381, pp.135–150.

Zhang, S., Zhang, Y., Liu, J., Xu, Q., Xiao, H., Wang, X., Xu, H. and Zhou, J., 2013. Thiol modified Fe_3O_4@SiO_2 as a robust, high effective, and recycling magnetic sorbent for mercury removal. *Chemical Engineering Journal*, 226, pp.30–38.